Received: 22 February 2023 | Revised: 12 April 2023 | Accepted: 16 April 2023

DOI: 10.1002/suco.202300124

ARTICLE

fib WILEY

A new *fib* Model Code proposal for a beam-end type bond test

Giovanni Metelli[1] | **John Cairns**[2] | **Giovanni Plizzari**[1]

[1]Department of Civil, Environmental, Architectural Engineering and Mathematics, University of Brescia, Brescia, Italy

[2]School of Energy, Geoscience, Infrastructure and Society, Heriot-Watt University, Edinburgh, UK

Correspondence
Giovanni Plizzari, Department of Civil, Environmental, Architectural Engineering and Mathematics, University of Brescia, via Branze 43, Brescia, Italy.
Email: giovanni.metelli@unibs.it

Funding information
Università degli Studi di Brescia

Abstract

A beam-end test is proposed in this paper and in the new *fib* Model Code 2020 to determine the effects of concrete type, confinement effects, and casting position on the anchorage strength of reinforcing bars. Two bars are cast in each specimen (in the two opposite corners), one in a "good" casting position and the other in "poor" casting position. The proposed test aims to be an economical bond test capable to represent actual conditions of anchored bars in real design practice. The test is also intended to verify whether existing provisions for bond and anchorage in the fib Model Code are suitable in nonconventional concrete. The validity of the proposed beam end type bond test is assessed by the results of more 60 tests on rebars having anchorage length of about 20 times the bar diameter in plain concrete, in fiber reinforced concrete, and in recycled aggregate concrete. Experimental results provide information both on the "top cast effect" in three types of concrete and on the effectiveness of *fib* Model Code provisions for anchorage when nonconventional concrete is used.

KEYWORDS

anchorages, bond in concrete, bond test, Model Code, top cast effect

1 | INTRODUCTION

Bond behavior affects several aspects of the performance of RC members. At serviceability limit states (SLS), crack spacing, crack width, beam deflection, and tension stiffening are all influenced by bond. At Ultimate Limit State (ULS), bond governs the capacity of anchorages and lap joints but bond also influences rotational capacity in plastic hinge regions, depending on yield penetration away from the crack.[1,2]

The capacity of anchorages and lap splices of rebars in concrete is a function of several factors as (1) the anchorage (or splice) length; (2) the resistance to splitting crack development provided by the concrete cover (including cover thickness and concrete tensile strength)[1,3–5]; (3) the bar diameter, because the size effect decreases the bond strength (BS) with increasing bar diameter[6]; (4) the rib geometry[7,8] which influences the interaction with the surrounding concrete; (5) the confinement provided by transverse reinforcement (if any) as links crossing the splitting surface[9–11]; (6) the transverse compression due to the reaction at the beam supports (when present); and (7) the casting position since, after pouring concrete, the mix water rises and large aggregates tend to drop down.[12,13] Therefore, near to the top surface, concrete may have lower mechanical properties due to its higher porosity and to the plastic settlement of concrete around the bars.

There are two principal modes of failure of anchorages and splices: (1) a pull-out type failure where the concrete shears across the top of the ribs and leaves a quite relative smooth bore where the bar has been pulled out; this is a relatively ductile failure; (2) a splitting failure with longitudinal cracks along the bar axis (provoked by the radial stresses generated by the ribs in the concrete cover), which can cause spalling of the cover. The splitting failure is the weaker of the two failure modes and generally occurs when the cover is less the 2.5–3.0 times the bar diameter.[1,3–5] This brittle failure can be controlled by transverse reinforcement crossing the potential splitting surface,[9,10] by the postcracking tensile strength of fiber-reinforced concrete (FRC),[14] or by transverse pressure (i.e., for anchorages at beam supports).[2]

As documented in the *fib* Bulletin 72,[15] the capacity of an anchorage or a lap may be evaluated with the formulation proposed in *fib* Model Codel 2010[16] which has been reformulated for design in the new MC2020 (Chapter 20).[17] This semi-empirical model was calibrated on the basis of test results on anchorages and laps having a length longer than 10 d_b in conventional concrete with a compressive strength ranging between 15 and 110 MPa. The arrival into the market of new types of concrete having mechanical and physical properties different from conventional concrete (such as FRC, recycled aggregate concrete [RAC], self-consolidating concrete, ultrahigh-performance concrete, etc.) as well as new types of rebars (including nonmetallic rebars) may require the development of specific design formulation of anchorages. At the same time, by considering the presence of different types of deformed bars into the market, it may be necessary to control the rebar bond performance; therefore, a reliable and practical bond test, representative of practical applications, should be adopted.

The standard tests available in international codes and standards or adopted by the research community differ significantly. In the pull-out test proposed by RILEM/CEB/FIP[18] and EN10080:2005,[19] the bar is in tension and the concrete is in compression. This (pull-out) test has been widely used because it is economical to manufacture and to test and because it represents the concept of bar anchoring. However, this configuration is not representative of any practical situation. Furthermore, the bar presents a short embedded length (5 d_b) which causes a quite uniform distribution of bond stresses along the bond length (while it varies in longer anchorages). Moreover, a large concrete cover (4.5 d_b, which is not representative for practice) and the friction arising at bottom bearing plate tends to confine the specimen, thus making the test not suitable to investigate splitting failure mode. It should be also noted that the stress developed by the bar is not directly proportional to the bond length; therefore, it is not possible to evaluate the capacity of real anchorages (where bond length typically exceeds 20 d_b) on the basis of the results of pull-out test with a short embedded length. Finally, pull-out specimen addresses only what would be classified in design Codes as a good casting location since good compaction of the concrete without voids around the bars is expected. The top cast (TC) ratio (the ratio between the bond strength of a bar near the top surface of a concrete element and that close to the bottom surface) tends to increase quite markedly as the bond length ratio (bond length divided by bar diameter) increases.[12] In fact, with a bond length equal to 5–10 times the bar diameter, the TC ratio is close to 0.5[12,13] while, for practical values of bond length, the TC ratio increases to one since the top bars tend to have a bond strength similar to the bottom bars.[12] Therefore, the investigated bond length significantly influences the test results.

An alternative test is the *beam test* proposed by RILEM/CEB/FIP,[18] adopted by EN 10080:2005,[19] prEN 10080:2023,[20] and by Eurocode 2.[21] In this test, the anchorage is placed in good bond condition close to the beam support where concrete is in tension, thus making the test more representative of actual conditions in structural elements. The bond length is 10 bar diameters (10 d_b, thus double than that of *pull-out test* but still not representative of practice) but the anchorage is characterized by a very high confinement of transverse reinforcement to avoid the shear failure of the beam specimen. In fact, the density of transverse reinforcement is about four times greater than that typical of practical design; therefore, the splitting failure of the anchorage, typical of real cases, is unlikely. The concrete cover is quasiconstant (minimum cover to the center of the bar is 50 mm), independent of the bar diameter; therefore, the cover to bar diameter ratio decreases with increasing bar size. Furthermore, in the *beam test*, the loaded end slip of the anchored bar (relevant for the crack widths and for tension stiffening) can be hardly measured. It should be also noted that it also is very difficult to handle the specimen during setting up the test because of its large dimensions (and weight) as well as the discontinuity at midspan (consequently manufacture of the specimens is not cost-effective). For all these reasons, the *beam test* cannot be used with sufficient degree of confidence to investigate all the parameters governing anchorage capacity. Furthermore, a wide experimental campaign showed a very limited correlation between RILEM *pull-out* and RILEM *beam end tests* (with a significant scatter of test results) because of the markedly different bond conditions.[22]

The potential purposes of a bond test were already identified and discussed in 2003 by Cairns and Plizzari.[23] These are mainly: (i) the routine quality control of

reinforcement; (ii) the performance classification for novel materials; (iii) the development of constitutive bond-slip laws for numerical analysis; (iv) the benchmarking of research studies and (v) the provision of design data. Cairns and Plizzari stated that the "principal purpose of a Standard bond test is to verify that a bar can be used with existing design guidance, itself derived from tests on situations representative of practical use."[23] This underlines that "Performance classification" is the main aim for a Standard bond test among all the possible functions listed above. It should be noted that a Standard bond test may also provide useful information and data for benchmarking of research studies, which can benefit from a *beam end test* representative of the actual behavior of anchorages.

Aim of this paper is to outline the format of an enhanced test method for bond and anchorages and to begin the process of calibration of the required structural performance.

2 | RESEARCH SIGNIFICANCE

A new *beam end test* is proposed in this paper and in the draft of Chapter 20 of the new Model Code 2020[17] that aims to improve the current Standard test procedures. The proposed standard bond test is mainly intended for "performance classification" of anchorages since the routine quality control of the ribbed bars can be adequately ensured by the measurement of the rib geometry after production as in EN ISO 15630-1:2019.[24] Moreover, it aims to be an economical bond test with limited dimensions but capable of representing actual conditions of anchored bars in real practice, and able to investigate the casting position effect. The proposed test method describes procedures to assess the anchorage capacity of steel reinforcing bars in concrete. This test may also be used to determine the limits of validity of the equations proposed in MC2020[17] since they were derived from a wide database collecting results from specimens made of conventional concrete. Thus, the proposed *beam end test* method is primarily intended to verify whether existing provisions for bond and anchorage in the *fib* Model Code are suitable also in non-conventional types of concrete; however, the proposed test may also be adopted to assess the performance of new types of reinforcement, especially when their geometries are not included in the existing standards.

The paper mainly focuses on the principles governing the design of a *beam end test* for the evaluation of anchorage capacity with an outline of the test setup specifications; however, the description does not aim to define all aspects for the purposes of a Standard. The effectiveness of the proposed *beam end test* is assessed through a wide experimental campaign for determining the anchorage capacity of steel rebars in plain concrete (PC), RCA, and FRC, which are nowadays often used in practical applications. The tests were carried out both at the University of Brescia (Italy) and at Heriot-Watt (Edinburgh, UK).

3 | A STANDARD BEAM END TEST

3.1 | Principle of the test

The principle of the test is to load a bar, that is cast into a concrete block representing the end section of a flexural element over a defined length, by a tensile force (F). The other end of the bar remains unstressed and a longitudinal equilibrating reaction is directly applied at the bottom portion of the specimen (Figure 1). In order to balance the overturning moment, two opposite vertical reactions R have to be applied to the specimen ends which allow a strut-and-tie mechanism to be developed in the block (Figure 1b) with the anchorage length set in the tensile portion of the concrete block and with an inclination of the compressive strut of about 45° (Figure 2).

The beam end specimen allows two bars to be tested in a single specimen. It is diagonally symmetric so that the second test can be done just by turning the specimen around. Two bars are arranged in the two opposite corners, in order to allow one bar to be tested in a "good" casting position and the other in a "poor" casting position at a distance of at least 300 mm from the bottom face, as defined in the draft MC2020[17] and in draft Eurocode 2.[25] The embedded length of the bar is set to a value dependent on the concrete compressive strength and steel grade and corresponds only to a part of the specimen length (Figure 2a). Since the *beam-end test* aims at verifying anchorage performance, the anchorage length is to be designed to develop a bar stress $f_{s,tgt}$ (as determined from Equation (2), proposed in *fib* MC2010[16]) of about 80% of the characteristic yield strength f_{yk}. Plastic sleeves (bond breakers) are placed at both bar ends ($>d_b$ and $> 5\ d_b$ at the loaded and unloaded bar ends, respectively) to control the position of the anchorage and to avoid a localized cone-type failure of the concrete at the loaded end of the specimen. The unbonded length at the free end aims to avoid the confinement provided by transverse pressure at the beam support (Figure 2a).

The bar to be tested extends beyond the length of the specimen. Displacement gauges are placed to both ends of the test bar for measuring the bar-to-concrete slip (i.e., the relative displacement between steel and concrete).

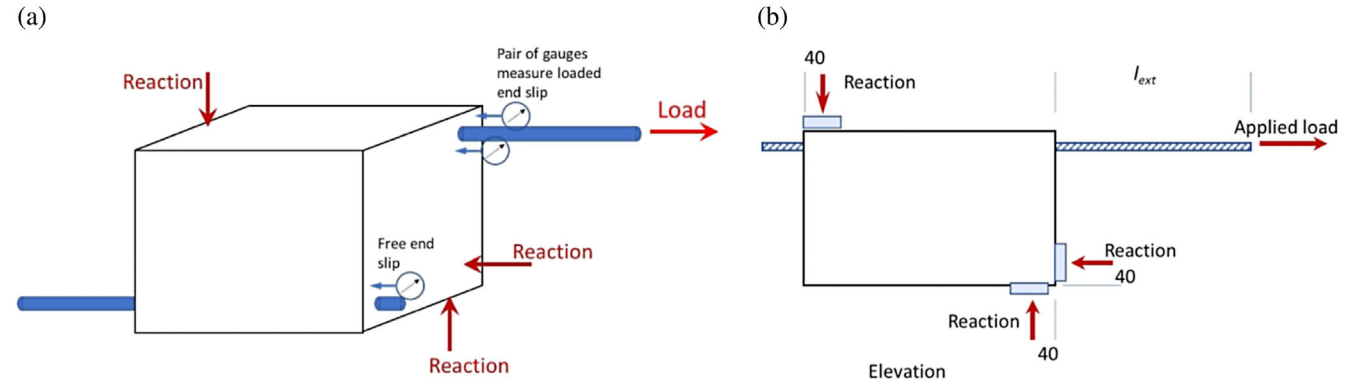

FIGURE 1 Schematic view of the beam end test specimen: position of the bars (a); applied load and reactions (b).

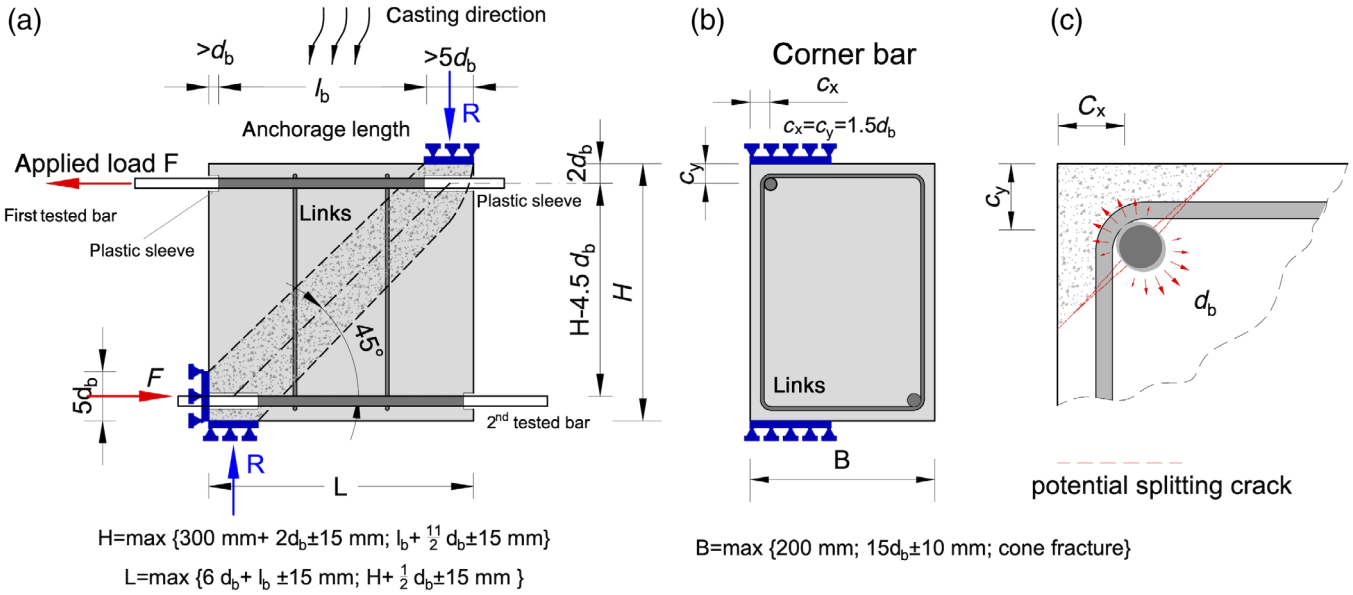

FIGURE 2 Beam end test specimen: longitudinal view (a); cross section and detailing of the concrete cover (b); splitting cracks at corner specimen (c).

The recommended concrete cover is equal to 1.5 d_b to represent common practical situations where splitting failure is expected prior yielding of the anchored bars (Figure 2b,c). Closed steel links are placed to provide transverse reinforcement within the range used in current practice, corresponding to a stirrups index of confinement (K_{tr})[16] of about 1%; the latter is defined as:

$$K_{tr} = n_t\, n_{st}\, A_{st}/(n_b\, d_b\, l_b) \quad (1)$$

where A_{st} is the area of the cross section of one leg (mm^2); n_{st} the total number of confining stirrups within the anchorage/lap length; n_t the number of legs of a stirrup crossing the potential splitting failure surface ($n_t = 1$ for corner bar); n_b is the number of anchored bars or pairs of lapped bars; d_b is the diameter of the bar (mm); and l_b is the lap/anchorage length (mm).

It should be noted that the general form of the *beam end test* proposed is similar to that proposed by ASTM 944:2015[26] where there is only a single bar placed at the midface of the bottom side with larger concrete cover (equal to 38 mm). As laps in beams may often be located in a "poor" casting position near the top of the concrete element, the Standard test should cover this condition as well. In the proposed *beam-end test*, the recommended location of the bar is at a corner (Figure 2b), where concrete confinement may be weaker but links are more effective; in the corner location, the bar shall be oriented with one set of ribs pointing towards the adjacent corner in order to favor a side-face splitting failure in the concrete block corner (Figure 2c).

In case of splitting failure of the anchorage, the maximum stress in the bar (f_{stm}) at anchorage (splitting) failure may be calculated with the semiempirical

formulation proposed by *fib* Model Code 2010[16] (Equation 2):

$$f_{stm} = 54\left(\frac{f_{cm}}{25}\right)^{0.25}\left(\frac{25}{d_b}\right)^{0.20}\left(\frac{l_b}{d_b}\right)^{0.55}[\alpha_2 + k_m K_{tr}] \quad (2)$$

where f_{cm} is the mean concrete compressive strength, d_b is the bar diameter, l_b is the anchorage length. In Equation (2), the maximum bar stress may benefit from the confinement contributions of concrete cover and transverse reinforcement as expressed by $\alpha_2 = [(c_{min}/d_b)^{0.25}(c_{max}/c_{min})^{0.10}]$ and by the stirrup index of confinement K_{tr}. The effectiveness factor of confining reinforcement is expressed by the factor k_m which depends on bar arrangements, varying between 12 and 0,[16] c_{max} and c_{min} are the largest and the smallest of: (i) one-half the clear spacing between anchored or lapped bars (c_s), (ii) bottom cover (c_y), and (iii) side cover (c_x), respectively. In the proposed *beam end test* with a corner bar, $\alpha_2 = 1.11$ since $c_{min} = c_x = c_y = 1.5\ d_b$ and $c_{max} = c_{min}$ while the effectiveness factor k_m is equal to 12 because the anchored bar is adjacent to the link crossing the potential splitting crack (see *fib* MC2010[16] and *fib* Bulletin 72[15] for further details). Setting parameters to these values appropriate to the proposed specimen leads to Equation (2a):

$$f_{stm} = 66\left(\frac{f_{cm}}{25}\right)^{0.25}\left(\frac{25}{d_b}\right)^{0.20}\left(\frac{l_b}{d_b}\right)^{0.55} \quad (2a)$$

Re-arranging Equation (2a) to determine the anchorage length gives Equation (3):

$$l_b = \left(\frac{f_{s,tgt}}{66}\right)^{1.8}\left(\frac{f_{cm}}{25}\right)^{-0.45}\left(\frac{25}{d_b}\right)^{-0.36} d_b \quad (3)$$

where $f_{s,tgt}$ is the target anchorage strength, set equal to $0.8\,f_{yk}$.

The height (H) and the length (L) of the specimen are set by assuming an inclination of the concrete strut of 45° and that the vertical reactions are applied beyond the anchorage length through bearing plates $5\ d_b$ long and 10 mm thick, over the width of the specimen (Figure 2a); a minimum distance of the top bar from the bottom surface of specimen of at least 300 mm shall be set in order to guarantee the "poor boor condition" of the top bar. Finally, the specimen width (B) may be set as the greater of $15\ d_b$ and 250 mm in order to avoid any interference between opposite bars in the failure mechanism as well as the concrete cone failure of the tensile portion of the block.

In summary, the specimen size should fit the following requirements:

$$H = \max\left\{\left(l_b + \frac{11}{2}d_b\right); (300 + 2\,d_b)\right\} \pm 15\,\text{mm} \quad (4a)$$

$$L = \max\{(l_b + 6\,d_b); (H + 0.5\,d_b)\} \pm 15\,\text{mm} \quad (4b)$$

$$B = \max\{15\,d_b; 250\,\text{mm}\} \pm 15\text{mm} \quad (4c)$$

In Figure 3a,b, the anchorage length and the specimen depth are plotted against the bar size for B500 and B700 steel grade, respectively, by varying the concrete strength from C25/30 to C70/80 and assuming the confinement factors from cover and reinforcement $\alpha_2 = 1.11$ and $\alpha_3 = 0.13$, respectively (being $\alpha_3 = k_m K_{tr}$ and $f_{cm} = f_{ck} + 8$ MPa). It should be noted that the specimen depth tends to increase more than linearly since the l_b/d_b ratio is not constant with the bar size; furthermore, the specimen depth is governed by the requirement for guaranteeing "poor bond condition" of the top bar when small bar size is used (Figure 3). For a bar size commonly used in beams and slabs (≤16 mm), the sizes of the beam end specimen are rather limited, thus making the specimen easy to manufacture and handle.

As an example, for a corner bar diameter of 16 mm and a target anchorage strength $f_{st,tgt} = 0.8\,f_{yk}$, an anchorage length of 308 mm ($l_b = 19.3\ d_b$) and a specimen depth of 400 mm ($H = 25\ d_b$) should be provided when using a C25/30 concrete and a B500 steel grade (Figure 3a).

Finally, it should be observed that the *beam end test* might also provide local bond properties between reinforcement and concrete when a shorter embedded length is used ($l_b \le 5\ d_b$); in this case, details for and transverse reinforcement, test setup to promote a pull-out failure may be found in[27] where the bond-slip law of reinforcement bars with different rib geometries is investigated.

3.2 | Preparation of samples

The test bar shall be in "manufactured" condition without losing mill scale, preferably entirely free from rust. If the test bar is corroded, the conditions of the bar shall be described in the test report and possibly supported by photographs of the surface. The bar shall not be cleaned in any way that might change its roughness.

The fresh concrete is cast vertically in the molds with the bars laid horizontally (Figure 2). Concrete shall be compacted and cured as specified by the mix designer in a manner consistent with the method proposed for practical use of the material.

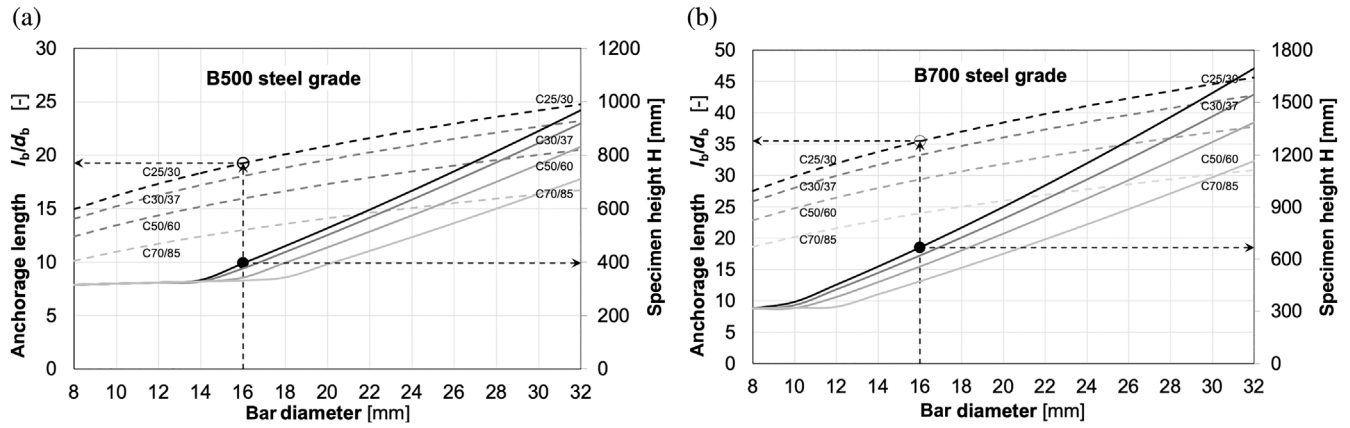

FIGURE 3 anchorage length l_b and height H of the beam end specimen versus bar size for B500 (a) and B700 (b) steel grade (corner bar with $c_x = c_y = 1.5\ d_b$).

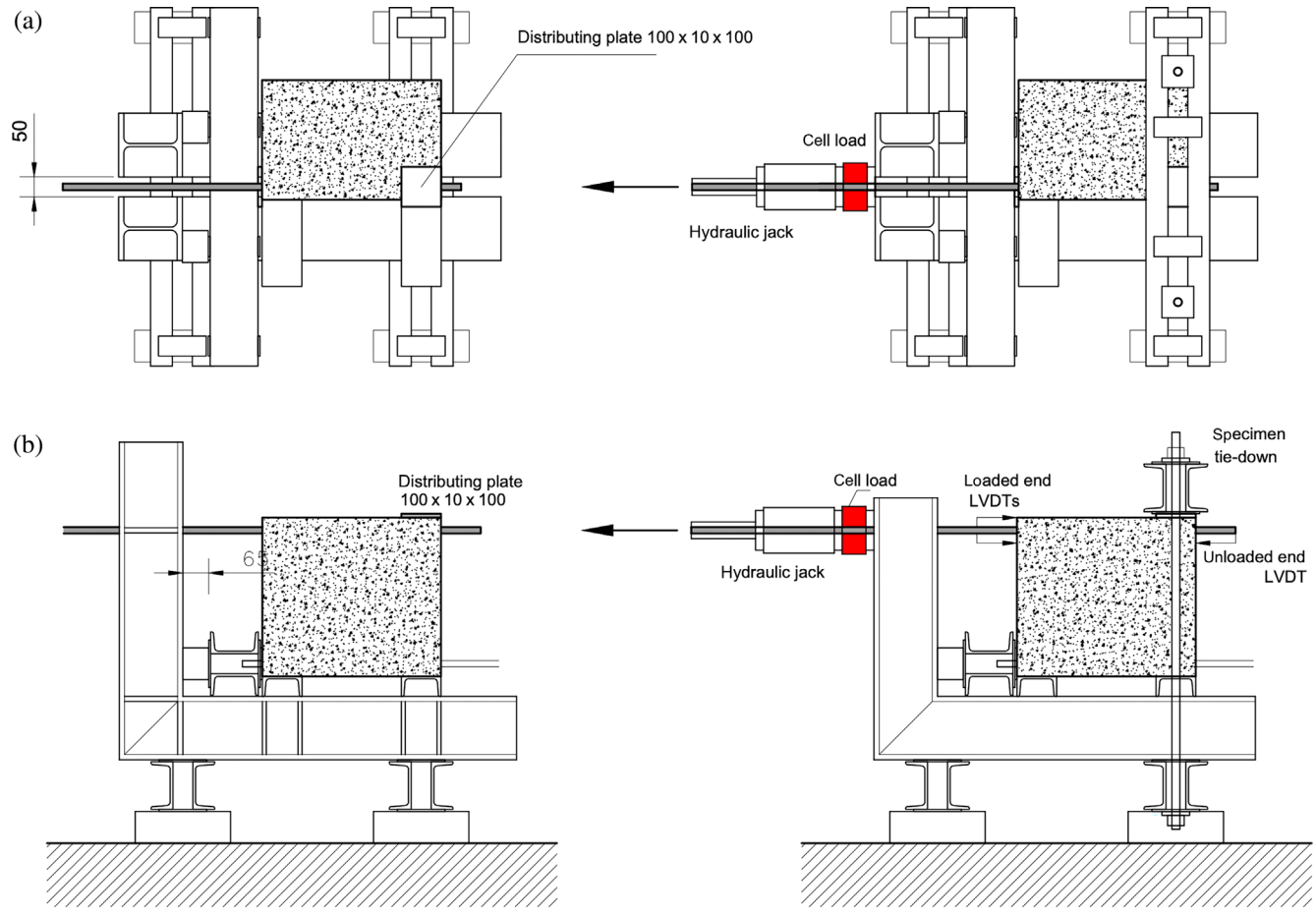

FIGURE 4 Typical test setup: plan view (a) and side elevation (b).

3.3 | Test setup

A sketch of a suitable test setup is shown in Figure 4. The top bar is pulled at one end while a bottom restrain prevents any longitudinal translation of the concrete block. The reacting bench may be a self-balanced frame consisting of two L-shaped rigid steel profiles simply supported by the floor. The steel bench should be stiff enough to ensure that the applied load remains parallel to the bar axis during testing. Two vertical ties connected by a transverse rigid steel beam are placed at the back of the specimen to avoid any rotation of the test block.

The loading system should be capable of measuring the applied tensile load (to an accuracy of ±2% of the applied force) by means of a load cell placed between the loading apparatus and the reacting steel bench (Figure 4). The compressive bottom portion of the specimen should be not greater than 5 d_b (corresponding to about 0.20 H). Displacements of the loaded end of the longitudinal bar are measured by two linear variable differential transformers (LVDTs) having an accuracy of 0.001 mm (Figure 4b) both positioned on a plane through the bar axis. One LVDT placed at the free end of the bar measures the unloaded end slip. Further measuring devices may be placed on the specimen side to monitor the crack opening and its propagation.

3.4 | Test procedure and interpretation of test results

Performance of the bar would be assessed by several measures, namely: peak bar stress ($f_{s,ex}$), bar stress at loaded end slip of 0.05 mm ($\delta_{L,0.05}$, relevant to crack width, tension stiffening, and beam deflection), free end slip at peak load ($\delta_{U,max}$), stress at unloaded end slip of 0.02 mm ($\delta_{uL,0.02}$, related to anchorage stiffness); diagrams of force or stress (f_s) versus free end slip (δ_U) relations shall be provided. Measured displacements at the loaded end have to be adjusted to take into account the elastic deformation of the bar outside the embedded length. The development of side and face splitting crack width (w_s and w_f, respectively) might be also checked both on the vertical and on top surface of the specimen, respectively.

4 | EXPERIMENTAL PROGRAM

The format of the proposed *beam end test* is assessed within two broad experimental programs carried out at the University of Brescia (Italy) and at Heriot-Watt University (Edinburgh, UK). The former is addressed at comparing the anchorage behavior and the casting position effect of steel rebars in PC with those in RAC and FRC having similar compressive strength. This experimental campaign consists of four batches with three samples each (24 tests). One bar diameter was investigated (16 mm) placed at corner location of the beam-end specimen with a 1.5 d_b concrete cover and an anchorage length of 20 d_b. The specimen was 450 mm long, 400 mm depth, and 300 mm wide (Figure 5). Two stirrups having a diameter of 6 mm are arranged along anchorage length ($K_{tr} = 1.1\%$). In the fourth series with RAC, three more specimens were tested with double transverse reinforcement ($K_{tr} = 2.2\%$) to allow the anchorage to reach the yield strength of the bar (about 450 MPa).

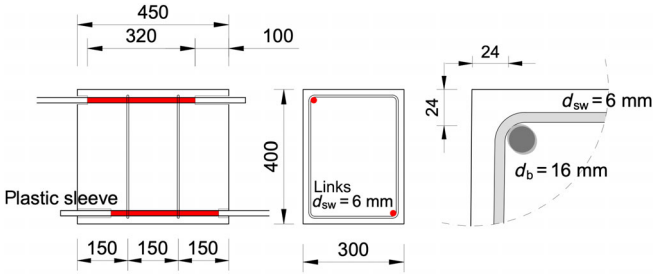

FIGURE 5 Dimensions of beam end specimens tested at the University of Brescia (Italy).

The experimental study carried out at Heriot-Watt University mainly aims at demonstrating the conformity of the proposed *beam-end test* to practical conditions by comparing results from beam-end tests with the mean anchorage strength determined according to Equation (2) from *fib* MC2010.[16] Two series consisting of 10 specimens were tested with either the bar in corner or center location (Figure 6). In the latter configuration, the anchorage strength may benefit from a higher concrete confinement with respect to the corner location, but the transverse reinforcing stirrups are less effective since the vertical links are not adjacent to the anchored bar.

In each series, two bar diameters are tested (10 and 16 mm) in normal strength concrete with the cover varying between 1.0 d_b and 3.1 d_b. The cross section of the beam-end specimen size was 200 × 300 mm and the length of the specimen was 280 mm for the 10 mm reinforcing bar and 400 mm for the 16 mm reinforcing bar. The embedded lengths of main bars were set as 18.5 d_b for a 10 mm and 19 d_b for a 16 mm bar. Stirrups with a diameter of 6 mm were provided at 100 mm spacing over the anchorage length, corresponding to two and three stirrups for 10 and 16 mm bar, respectively (stirrup index of confinement of 3.06% and 1.74%).

Table 1 exhibits all the geometrical and mechanical properties of the specimens, namely: concrete cover, anchorage length, diameter and number of the confining links and the stirrups index of confinement along with the maximum stress in the bar (f_{stm}) determined according to the MC2010 semiempirical equation (Equation 2) by assuming a concrete compressive-strength target $f_{cm} = 33$ MPa.

4.1 | Material properties

Steel grade B500C (according to EN 10080[19]) was used for all types of reinforcement. The 16 mm rebars tested in

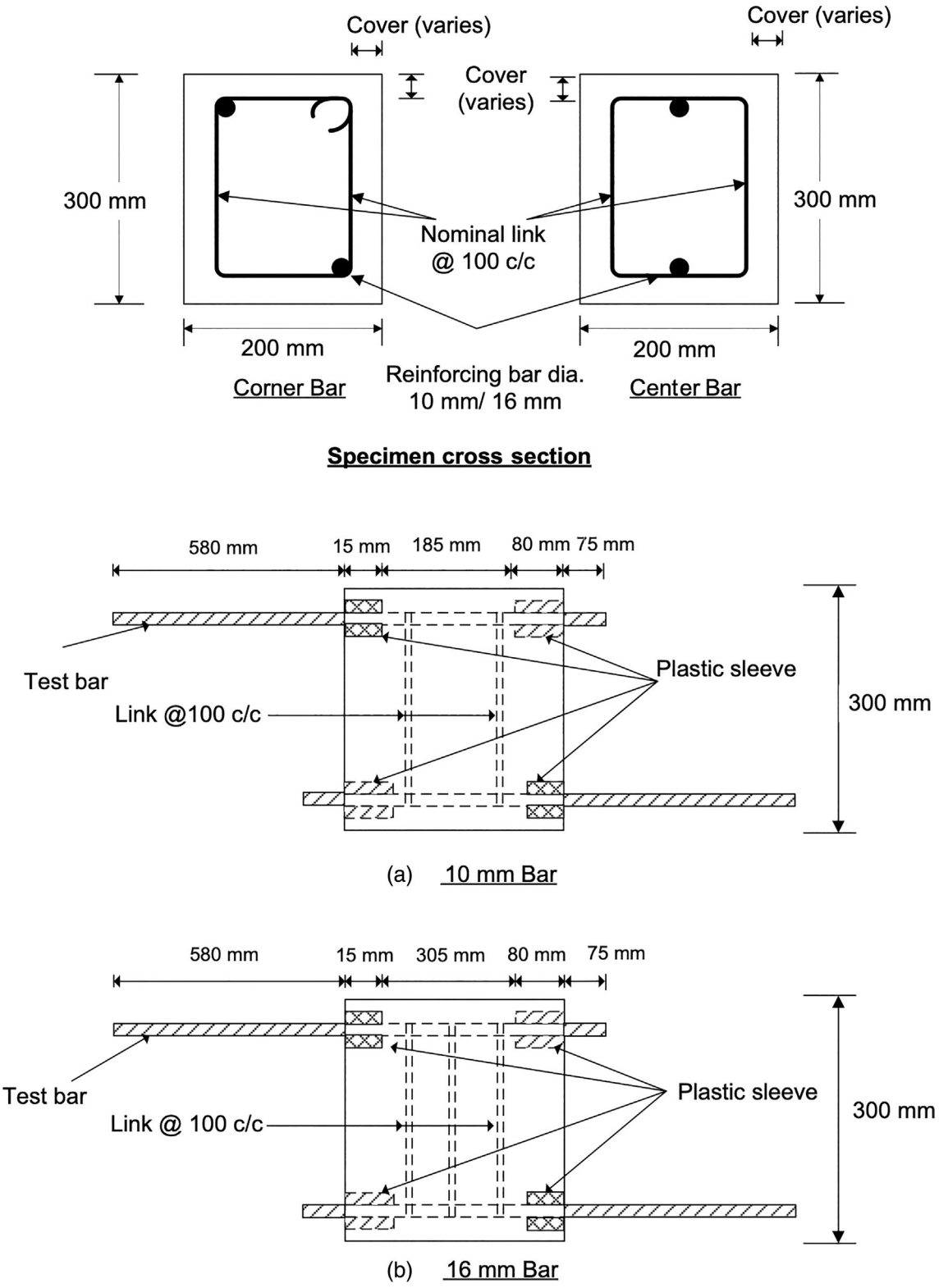

FIGURE 6 Dimensions of beam end specimens testes at the Heriot-Watt University (UK).

Italy had a relative rib area $f_r = 0.079$ and mean yield strength $f_{ym} = 526$ MPa while those used in United Kingdom had a $f_r = 0.07$ or 0.08 and a $f_{ym} = 570$ and 560 MPa, for 10 and 16 mm rebars, respectively. The same mix design was used for the reference PC and FRC mixtures (Table 2) tested in Italy, both with a target concrete class of C25/30; the concrete was supplied by local ready-mix company. Hooked-end steel fibers

TABLE 1 Geometrical and mechanical properties of the tested anchorages.

	Series			N (−)	d_b (mm)	l_b/d_b [−]	c_x (mm)	c_y (mm)	α_2 (−)	d_{sw} (mm)	n_t (−)	n_{st} (−)	K_{tr} (%)	a_l (mm)	k_m (−)	f_{stm} (MPa)	f_{stm}/f_{yk} (−)
University of Brescia (Italy)	1	PC	C	3	16	20	24	24	1.11	6	1	2	1.10	0	12	407	0.81
	2	FRC	C	3	16	20	24	24	1.11	6	1	2	1.10	0	12	407	0.81
	3	RAC	C	3	16	20	24	24	1.11	6	1	2	1.10	0	12	407	0.81
	4	RAC	C	3	16	20	24	24	1.11	6	1	4	2.21	0	12	451	0.90
Heriot-Watt (UK)	5	PC	C	1	10	18.5	22	22	1.22	6	1	2	3.06	0	12	529	1.06
		PC	C	1	10	18.5	31	31	1.33	6	1	2	3.06	0	12	565	1.13
		PC	C	1	10	18.5	16	16	1.12	6	1	2	3.06	0	12	498	1.00
		PC	C	1	10	18.5	25	25	1.26	6	1	2	3.06	0	12	542	1.08
		PC	C	1	16	19	22	22	1.08	6	1	3	1.74	0	12	414	0.83
		PC	C	1	16	19	31	31	1.18	6	1	3	1.74	0	12	445	0.89
		PC	C	1	16	19	46	46	1.30	6	1	3	1.74	0	12	484	0.97
		PC	C	1	16	19	16	16	1.00	6	1	3	1.74	0	12	387	0.77
		PC	C	1	16	19	25	25	1.12	6	1	3	1.74	0	12	425	0.85
		PC	C	1	16	19	40	40	1.26	6	1	3	1.74	0	12	469	0.94
	6	PC	Ce	1	10	18.5	95	22	1.41	6	2	2	6.11	73	0	470	0.94
		PC	Ce	1	10	18.5	95	31	1.48	6	2	2	6.11	64	0	495	0.99
		PC	Ce	1	10	18.5	95	16	1.34	6	2	2	6.11	79	0	448	0.90
		PC	Ce	1	10	18.5	95	25	1.44	6	2	2	6.11	70	0	479	0.96
		PC	Ce	1	16	19	92	22	1.25	6	2	3	3.48	70	12	534	1.07
		PC	Ce	1	16	19	92	31	1.32	6	2	3	3.48	61	12	555	1.11
		PC	Ce	1	16	19	92	46	1.40	6	2	3	3.48	46	12	580	1.16
		PC	Ce	1	16	19	92	16	1.19	6	2	3	3.48	76	12	515	1.03
		PC	Ce	1	16	19	92	25	1.27	6	2	3	3.48	67	12	541	1.08
		PC	Ce	1	16	19	92	40	1.37	6	2	3	3.48	52	12	571	1.14

Note: a_l, distance of the anchored bar to the link; C, corner bar; Ce, central bar; c_x, c_y, side and vertical concrete cover; d_{sw}, stirrup diameter; $f_{cm} = 33$ MPa; f_{stm} bar stress estimated with Equation (2); K_{tr}, stirrup index of confinement; N, number of tested specimens; n_t, n_{st}, number of transversal legs and transversal reinforcement; α_2, confinement coefficient provided by concrete cover (as expressed by MC2010).
Abbreviations: FRC, fiber-reinforced concrete; PC, plain concrete; RAC, recycled aggregate concrete.

TABLE 2 Mixture proportions of FRC and RAC.

Plain or FRC		RAC	
Cement content CEM I-32-5R (kg/m^3)	320	Cement content CEM 32.5 II/B-LL (kg/m^3)	320
Water (L/m^3)	155	Water (L/m^3)	165
Water/cement ratio (−)	0.48	Water/cement ratio (−)	0.52
Sand (0/2 mm) (kg/m^3)	183	Sand (0/2 mm) (kg/m^3)	204
Sand (0/6 mm) (kg/m^3)	568	Sand (2/6 mm) (kg/m^3)	593
Coarse aggregate (6/14 mm) (kg/m^3)	906	Coarse aggregate (6/20 mm) (kg/m^3)	473
Gravel (15/30) (kg/m^3)	224	Gravel (20/32) (kg/m^3)	226
Max. aggregate dimension (mm)	22.4	Max. aggregate dimension (mm)	32
Fibers (kg/m^3)	40	Recycled aggregate (8/22 mm) (kg/m^3)	510
V_f (%)	0.5	— (%)	—
Superplasticizer (L/m^3)	6.0	Superplasticizer (L/m^3)	5.0

Abbreviations: FRC, fiber-reinforced concrete; RAC, recycled aggregate concrete.

($L_f = 60$ mm, $d_f = 0.40$ mm with a tensile strength of 1200 MPa) were used with a volume fraction of 0.5% (corresponding to about 40 kg/m^3). PC had a slump of 220 mm, whereas FRC had a lower slump (170 mm, measured according to EN 12350-2[28]), due to the addition of fibers. Six standard 150 mm cube control specimens were used for each mixture to evaluate the concrete compressive strength. Cubes were cured in the laboratory until testing the beams. At the time of the bond tests, the PC and FRC specimens had an average cube compressive strength ($f_{cm,cube,ex}$) of about 36 MPa. The postcracking tensile strength of FRC, determined according to EN14651[29] was characterized by the following parameters: $f_{R1m} = 7.18$ MPa and $f_{R3m} = 7.65$ MPa.

The RAC was supplied by a ready-mix company with a C25/30 target class. In RAC, the water–cement ratio was 0.52 and 25% of natural coarse aggregate was replaced by recycled aggregate having a diameter ranging between 8 and 22 mm (Table 2). The latter was obtained from blast furnace slags, whose density ranges between 3100 and 3250 kg/m^3. At the time of the bond tests, the RAC had an average compressive cube strength ($f_{cm,cube,ex}$) of about 40 MPa (determined on 20 cube specimens). The slump of RAC was 170 mm (S4 workability class).

In Series 5 and 6 tested in the United Kingdom, PC had an average cube compressive strength of 40.6 or 44.9 MPa.

4.2 | Discussion of test results

The main experimental results of Series 1–4 are listed in Table 3 where maximum load (P_u), maximum bar stress ($f_{s,ex}$), maximum unloaded end slip ($\delta_{UL,max}$), bar stress at a loaded end slip of 0.05 mm ($f_{s,\delta L0.05}$) and at free end slip of 0.02 mm ($f_{s,\delta UL0.02}$) are reported for each specimen along with the secant stiffness ($K_{UL0.02}$) of the anchorage measured at free end slip of 0.02 mm. In Series 5 and 6, only the peak load at failure was recorded (Table 4).

Figure 7 shows the comparison of the bar stress ($f_{s,ex}$) versus unloaded-end slip (δ_{UL}) curves between top and bottom anchorages for each series. The curves clearly show higher bar stresses and a stiffer behavior of bars in bottom location where good bond conditions are expected. None of the specimens showed any descending postpeak behavior, confirming the brittle behavior of anchorages with low confinement of transverse reinforcement (without transverse pressure). At the same time, it should be observed that top anchorages exploited larger unloaded end slip at peak load. This effect increases with the value of the stirrup index of confinement (K_{tr}), as expected in Series 4 (Figure 7) where the amount of confining transverse reinforcement, which was doubled with respect to the other series, allowed a better control of the propagation of the splitting cracks.

As far as the failure mode is concerned, most of specimens failed because of the development of side-face splitting crack which quickly developed from the loaded end towards the free end (Figure 8a). However, the anchorage in bottom location of PC_2 specimen and all bottom anchorages in RAC of Series 4, presented a mixed failure mode with both a concrete cone at the loaded end and longitudinal splitting cracks (Figure 8b). Finally, in the specimen FRC_1 the bottom anchored bar yielded.

4.2.1 | Anchorage strength.

In order to better compare the performance of the anchorages, the maximum nominal bar stress measured

TABLE 3 Test results of Series 1–4.

Specimen	d_b (mm)	f_{cm} (MPa)	f_{stm} (MPa)	P_u (kN)	$f_{s,ex}$ (MPa)	$\delta_{UL,max}$ (mm)	$f_{s\delta L,0.05}$ (MPa)	$f_{s\delta UL,0.02}$ (MPa)	$K_{UL0,02}$ (MPa/mm)	*BS* (–)	*TC* (–)	Failure mode
Series 1—PC												
PC_1_top	16	29.9		54.1	269.0	0.09	81.04	247.9	12.4	0.68	0.73	SP
PC_2_top	16	29.9		64.5	320.9	0.05	118.8	307.9	15.4	0.81	0.81	SP
PC_3_top	16	29.9		63.8	317.1	0.11	182.1	279.9	14.0	0.80	0.84	SP
Mean value				60.8	302.3	0.08	127.3	278.6	13.9	0.76	0.79	
(cv)				10%	10%	36%	40%	11%	11%	10%	7%	
PC_1_bot	16	29.9	397	73.6	366.2	0.05	191.2	321.0	16.1	0.92	—	SP
PC_2_bot	16	29.9	397	80.1	398.2	0.07	230.8	382.8	19.1	1.00	—	Co-SP
PC_3_bot	16	29.9	397	76.2	378.8	—	202.5	—	—	0.95		SP
Mean value				76.6	381.1	0.06	208.2	351.9	17.6	0.96		
(cv)				6%	4%	25%	10%	12%	12%	4%		
Series 2—FRC												
FRC_1_top	16	29.9		99.7	495.8	0.74	39.20	383.3	19.2	1.25	0.93	SP
FRC_2_top	16	29.9		73.0	363.1	—	—	—	—	0.91	0.92	SP
FRC_3_top	16	29.9		69.0	343.2	0.59	158.8	269.4	13.5	0.86	0.67	SP
Mean value				80.6	400.7	0.67	99.0	326.3	16.3	1.01	0.84	
(cv)				21%	21%	15%	85%	25%	25%	21%	18%	
FRC_1_bot	16	29.9	397	107.1	532.8	0.37	83.3	517.8	25.9	1.34	—	Y
FRC_2_bot	16	29.9	397	79.4	394.8	0.54	28.8	362.0	18.1	0.99	—	SP
FRC_3_bot	16	29.9	397	103.4	514.2	—	224.2	—	—	1.30		SP
Mean value				96.6	480.6	0.45	112.1	439.9	22.0	1.21		
(cv)				16%	16%	26%	90%	25%	25%	16%		

(Continues)

TABLE 3 (Continued)

Specimen	d_b (mm)	f_{cm} (MPa)	f_{stm} (MPa)	P_u (kN)	$f_{s,ex}$ (MPa)	$\delta_{UL,max}$ (mm)	$f_{s\delta L,0.05}$ (MPa)	$f_{s\delta UL,0.02}$ (MPa)	$K_{UL0,02}$ (MPa/mm)	*BS* (−)	*TC* (−)	Failure mode
Series 3—RAC												
RAC_1_top	16	33.2		50.8	252.6	0.20	144.3	214.0	10.7	0.62	0.62	SP
RAC_2_top	16	33.2		50.5	251.3	0.06	86.6	248.0	12.4	0.62	0.61	SP
RAC_3_top	16	33.2		39.4	195.9	0.16	75.6	162.0	8.1	0.48	0.56	SP
Mean value				46.9	233.3	0.14	102.2	208.0	10.4	0.57	0.59	
(cv)				14%	14%	50%	36%	21%	21%	14%	5%	
RAC_1_bot	16	33.2	408	82.5	410.5	0.09	261.3	408.2	20.4	1.01	—	SP
RAC_2_bot	16	33.2	408	82.7	411.5	0.06	152.3	408.0	20.4	1.01	—	SP
RAC_3_bot	16	33.2	408	70.7	351.6	0.03	88.4	332.8	16.6	0.86		SP
Mean value				78.7	391.2	0.06	167.3	383.0	19.2	0.96		SP
(cv)				9%	9%	45%	52%	11%	11%	9%		
Series 4 – RAC												
RAC_1_top	16	33.2		58.7	291.9	0.52	158.51	183.5	9.2	0.65	0.64	SP
RAC_2_top	16	33.2		54.1	269.3	0.64	66	104.3	5.2	0.60	0.59	SP
RAC_3_top	16	33.2		52.5	261.2	0.75	96.32	137.4	6.9	0.58	0.66	SP
Mean value				55.1	274.1	0.63	106.9	141.7	7.1	0.61	0.63	
(cv)				6%	6%	18%	44%	28%	28%	6%	6%	
RAC_1_bot	16	33.2	452	92.0	457.7	0.06	126.5	425.0	21.3	1.01	—	Co-SP
RAC_2_bot	16	33.2	452	92.5	460.1	0.08	171.4	430.1	21.5	1.02	—	Co-SP
RAC_3_bot	16	33.2	452	79.2	393.9	0.06	240.8	351.3	17.6	0.87		Co-SP
Mean value				87.9	437.2	0.07	179.6	402.1	20.1	0.97		
(cv)				9%	9%	13%	32%	11%	11%	9%		

Abbreviations: BS, bond strength ratio; Co, cone failure; FRC, fiber-reinforced concrete; PC, plain concrete; RAC, recycled aggregate concrete; SP, splitting of concrete cover; TC, top cast ratio; Y, bar yielding.

TABLE 4 Test results of Series 5 and 6.

Series	Position		d (mm)	c (mm)	f_{cm} (MPa)	f_{stm} (MPa)	P (kN)	$f_{s,ex}$ (MPa)	BS (−)	TC (−)	Failure mode
5	C	Top	10	22	37.4	546	29.0	369	0.68	0.70	SP
	C	Top	10	31	37.4	583	31.3	399	0.68	0.63	SP
	C	Top	10	16	33.8	501	21.5	274	0.55	0.49	SP
	C	Top	10	25	33.8	545	28.3	360	0.66	0.58	SP
	C	Top	16	22	37.4	427	73.4	365	0.86	0.90	SP
	C	Top	16	31	37.4	459	82.0	408	0.89	0.94	SP
	C	Top	16	46	37.4	499	86.3	429	0.86	0.83	SP
	C	Top	16	16	33.8	389	53.6	267	0.69	0.61	SP
	C	Top	16	25	33.8	427	67.7	337	0.79	0.64	SP
	C	Top	16	40	33.8	472	105.6	525	1.11	0.80	SP
							Mean value (cv)		0.78 21%	0.71 21%	
	C	Bottom	10	22	37.4	546	41.1	524	0.96		SP
	C	Bottom	10	31	37.4	583	50.0	637	—		Y
	C	Bottom	10	16	33.8	501	43.5	554	1.11		SP
	C	Bottom	10	25	33.8	545	48.5	618	—		Y
	C	Bottom	16	22	37.4	427	81.8	407	0.95		SP
	C	Bottom	16	31	37.4	459	87.5	435	0.95		SP
	C	Bottom	16	46	37.4	499	103.5	515	1.03		SP
	C	Bottom	16	16	33.8	389	88.6	441	1.13		SP
	C	Bottom	16	25	33.8	427	105.8	526	1.23		SP
	C	Bottom	16	40	33.8	472	131.2	653	—		Y
							Mean value (cv)		1.05 14%		
6	Ce	Top	10	22	34.5	485	40.5	516	1.06	0.91	SP
	Ce	Top	10	31	37.4	511	38.0	484	0.95	0.81	SP
	Ce	Top	10	16	33.8	451	35.0	446	0.99	0.69	SP
	Ce	Top	10	25	33.8	482	35.4	451	0.94	0.76	SP
	Ce	Top	16	22	37.4	551	73.9	368	0.67	0.73	SP
	Ce	Top	16	31	37.4	572	74.9	373	0.65	0.78	SP
	Ce	Top	16	46	37.4	599	89.2	444	0.74	0.86	SP
	Ce	Top	16	16	33.8	518	66.1	329	0.63	0.60	SP
	Ce	Top	16	25	33.8	545	76.5	380	0.70	0.69	SP
	Ce	Top	16	40	33.8	575	82.1	409	0.71	0.67	SP
							Mean value (cv)		0.80 20%	0.75 13%	
	Ce	Bottom	10	22	34.5	485	44.4	565	1.16		SP
	Ce	Bottom	10	31	37.4	511	46.8	596	—		Y
	Ce	Bottom	10	16	33.8	451	50.8	647	—		Y
	Ce	Bottom	10	25	33.8	482	46.8	596	—		Y
	Ce	Bottom	16	22	37.4	551	101.8	506	0.92		SP
	Ce	Bottom	16	31	37.4	572	95.8	477	0.83		SP
	Ce	Bottom	16	46	37.4	599	103.5	515	0.86		SP
	Ce	Bottom	16	16	33.8	518	109.7	546	1.05		SP
	Ce	Bottom	16	25	33.8	545	111.0	552	1.01		SP
	Ce	Bottom	16	40	33.8	575	122.9	612	—		Y
							Mean value (cv)		0.97 13%		

Abbreviations: BS, bond strength ratio; Co: cone failure; C: corner; Ce: center; SP, splitting of concrete cover; TC, top cast ratio; Y, bar yielding.

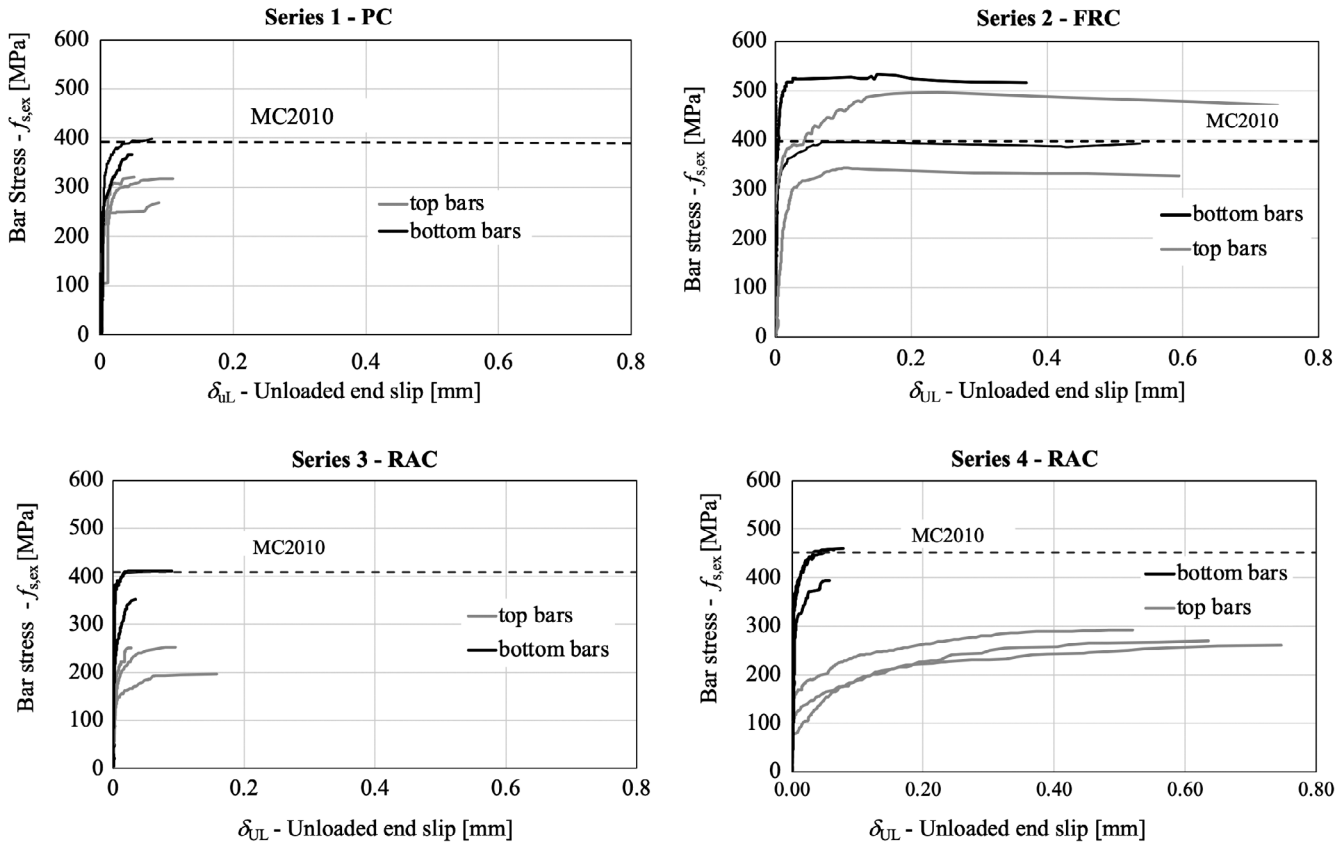

FIGURE 7 Test results of Series 1–4; bar stress $f_{s,ex}$ versus unloaded end slip δ_{UL} (in Series 2 the unloaded end slip of FRC_2-bottom is missing for recording error). FRC, fiber-reinforced concrete; PC, plain concrete; RAC, recycled aggregate concrete.

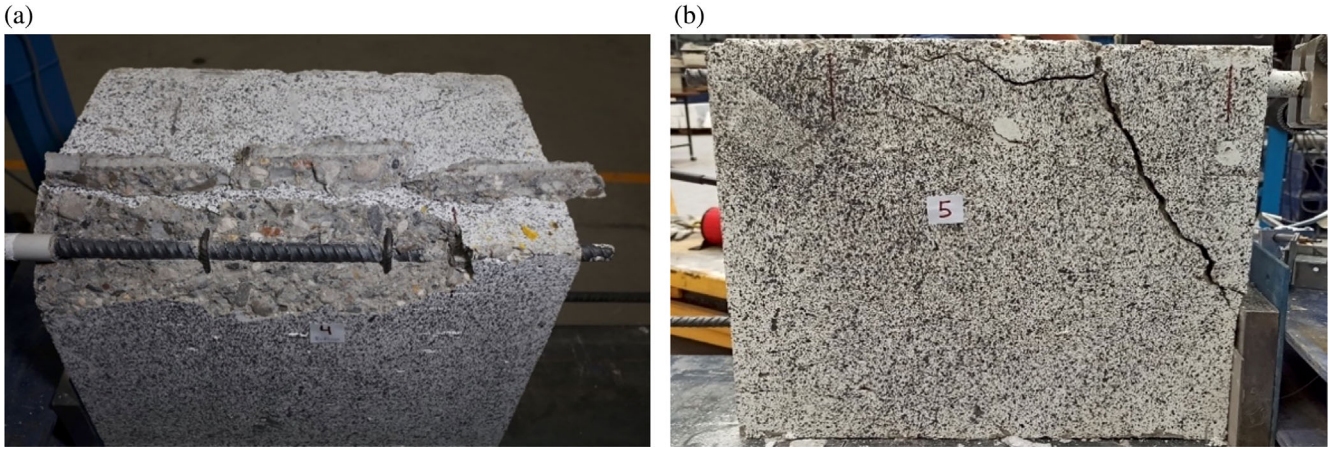

FIGURE 8 Splitting failure (a) and mixed failure mode with concrete cone blowing off (b).

in the test ($f_{s,ex}$) is normalized to the mean bar stress determined according to the MC2010 formulation (Equation 2); this provides a better comparison between experimental results and code prediction among specimens having different concrete strength and confinement from stirrups and concrete cover. The main test results along with the BS ratio ($BS = f_{s,ex}/f_{stm}$) and the TC ratio (expressed as the ratio between the maximum bar stress developed by a top bar with respect with that measured in the corresponding bottom cast one, $TC = f_{s,ex}{}^{top} / f_{s,ex}{}^{bot}$) are reported in Tables 3 and 4.

In Figure 9a, the mean *BS* ratio is depicted for top and bottom bars of each series. For the bottom bars, the *BS* ratio ranges between 0.96 and 1.05 in PC (Series 1, 5,

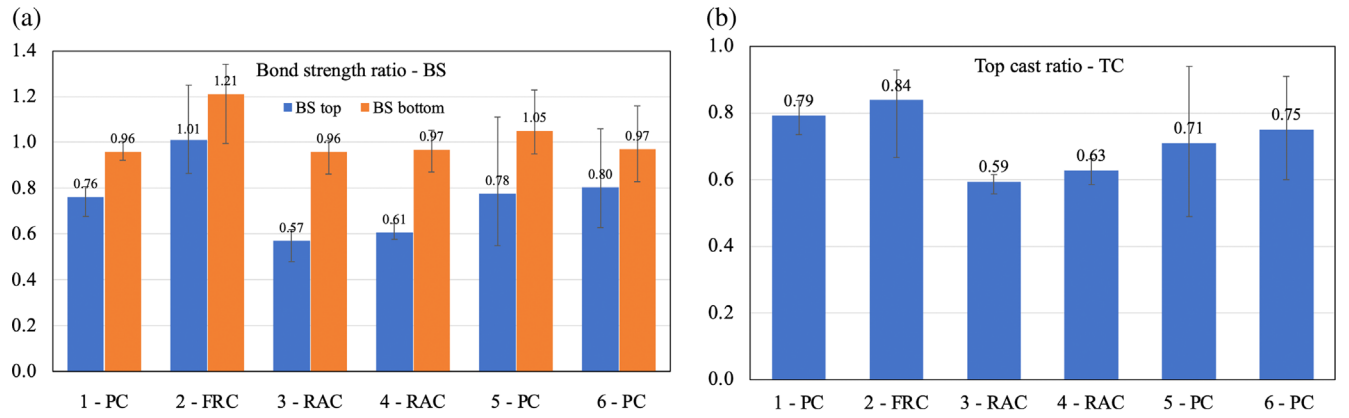

FIGURE 9 Bond strength (BS) ratio (a) and top cast (TC) ratio (b). FRC, fiber-reinforced concrete; PC, plain concrete; RAC, recycled aggregate concrete.

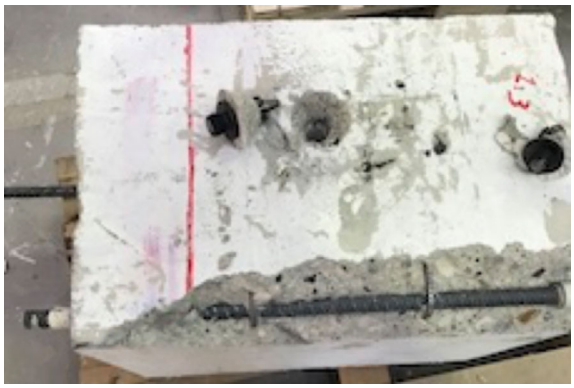

FIGURE 10 Pull-out test on concrete cover of a RAC specimen.

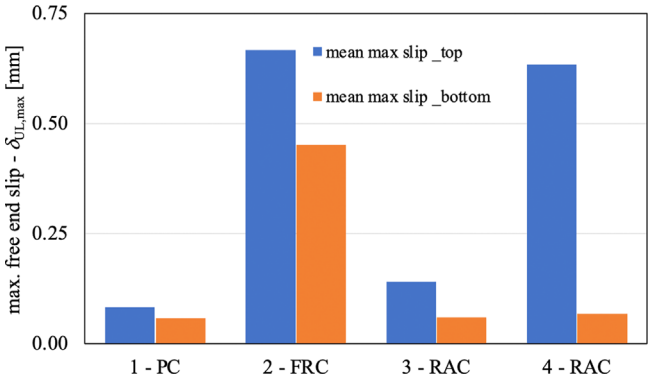

FIGURE 11 Maximum unloaded end slip measured in Series 1–4. FRC, fiber-reinforced concrete; PC, plain concrete; RAC, recycled aggregate concrete.

and 6) with a coefficient of variation lower than 14%; in RAC (Series 3 and 4), BS ratio is 0.96, while it is >1 only in Series 2 concerning FRC specimens, thus confirming the beneficial effect of confinement provided by FRC postcracking strength on the anchorage strength. The experimental BS ratio of PC specimens confirm the reliability of the MC2010 formulation (Equation 2) to predict the anchorage strength. However, the *BS* ratio decreased to 0.76 and to about 0.6 for the top bars in PC and RAC, respectively; this result evidences the influence of bleeding and of plastic settlement of fresh concrete (casting position effect) on the anchorage strength of bars cast near the top of a pour. The mean TC ratio of each series is reported in the histogram of Figure 9b, which evidences the strength reduction for top bars with respect to the bottom ones. The decrease of the anchorage resistance ranges between 29% and 21% in PC while it is 16% in FRC. A significant decrease of anchorage strength in poor casting position is measured for RAC (40%) which may be due to the density of recycled aggregates derived from blast furnace slags (BFS) that was 15% greater than that of the natural gravel. This difference may lead to a higher percentage of BFS aggregates in the lower part of the specimen. This kind of segregation may have caused different mechanical properties between the bottom and the top portion of the concrete element.

This different strength was confirmed by two pull-out tests on concrete cover (measured according to EN 1250-4-3[30]) which provided a concrete strength of 33 and 16 MPa, of the bottom and top cover of specimen RAC_1, respectively (Figure 10). This result suggests that the replacement of fine and coarse natural aggregate with BFS in RAC should be adequately proportioned to avoid any concrete segregation.

The experimental campaign provides also useful results on the brittleness of the anchorages in different concrete typologies, both in poor and good casting condition. In Figure 11, the maximum unloaded end slip ($\delta_{UL,max}$) of the anchorages in top or in bottom locations is plotted for each series. A markedly less brittle behavior of bars in top location can be seen: the maximum end slip reaches a value close to 0.7 mm when transverse

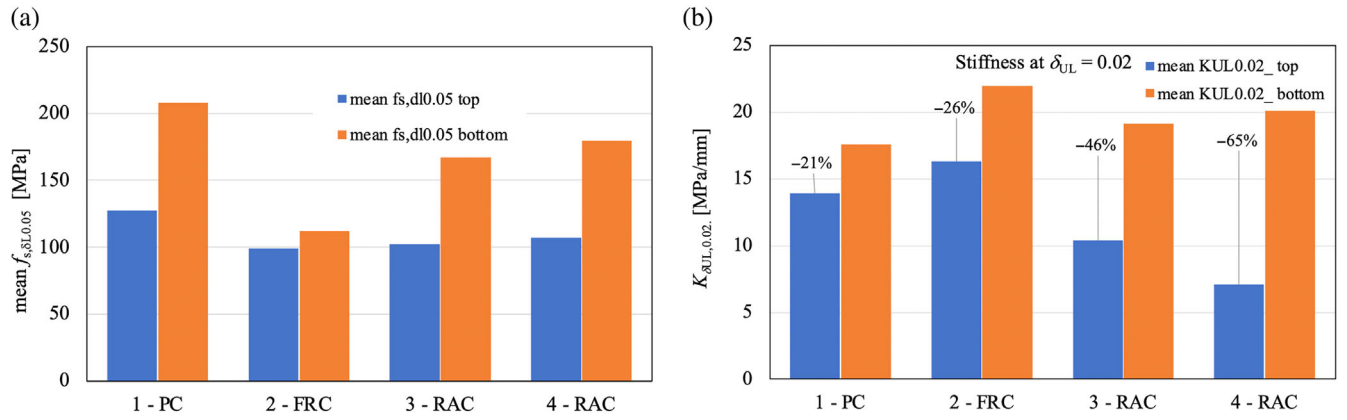

FIGURE 12 Mean bar stress at a loaded end slip of 0.05 mm (a); anchorage stiffness measured at an unloaded end slip of 0.02 mm (b). FRC, fiber-reinforced concrete; PC, plain concrete; RAC, recycled aggregate concrete.

confinement is provided by steel fibers (Series 2) or by doubling the stirrups index of confinement (Series 4). The capability of FRC to control the anchorage failure can be observed also for anchorages in bottom location, since the maximum free end slip is five times greater than that of anchorages in PC.

4.2.2 | Anchorage stiffness

Finally, the performance of anchorage behavior at SLS (related to crack width control) can be expressed by the bar stress ($f_{s,\delta L0.05}$) at a loaded end slip of 0.05 mm. To this aim, in Figure 12a the mean value of the bar stress of each series is plotted both for top and bottom location. First, it should be noted that the bar stress is never >240 MPa, as required at SLS to control the crack width.[21] Furthermore, the top anchorages show a markedly softer behavior (with a decrease between 32% and 41% of the stiffness) with respect to the bottom bars. However, the test results present a large scatter with a coefficient of variation even >50% (Table 3).

A lower scatter of the anchorage stiffness can be obtained when measuring the bar stress ($f_{s,\delta UL0.02}$) at an unloaded end slip of 0.02 mm (coefficient of variation ≅ 11% in Series 1, 3, and 4, and ≅ 28% in Series 4). The secant stiffness $K_{\delta UL,0.02}$ of the bar stress ($f_{s,ex}$) versus slip (δ_{UL}) curve at an unloaded end slip of 0.02 mm is plotted in Figure 12b; it should be noted that the casting position also affects the anchorage stiffness of top bars with a decrease of 21% and 26% in PC and FRC, respectively, when compared with bottom ones. As already observed for the anchorage strength, the stiffness reduction is greater in RAC (equal to 46% and 65% in Series 3 and 4, respectively). These results may support the assumption of a more uniform distribution of bond stress in top location, which may mitigate the casting position effect in long anchorages/laps.[12]

5 | CONCLUDING REMARKS

This paper outlines a beam end test that is particularly useful to verify the applicability of existing provisions for bond and anchorage in the *fib* Model Code when using nonconventional concrete; however, the proposed test may also adopted for assessing the performance of new types of reinforcement.

After presenting and discussion the geometry of the new beam-end specimen, experimental results of 64 tests of long anchorages of steel ribbed bars in different types of concrete (PC, FRC, and RAC) are presented. The tests were carried out in two different laboratories.

Based on the test results, the following remarks can be made:

1. The proposed bond test is cost-effective with limited dimensions and easy handling; this test is capable to represent actual conditions of anchored bars in real design practice and it allows the casting position effect to be better investigated;
2. The tests results confirm the reliability of the MC2010 formulation to predict the strength of long anchorages, and hence its viability to serve as the basis for the design of the anchorage length to be used in a standardized bond test;
3. Anchorages having a length of about 20 times the bar diameter show a strength reduction of about 25% in top location with respect to the bottom one in normal strength concrete;
4. The use of FRC leads to a significant increase in the anchorage strength and a slight reduction of the TC effect with respect to PC;
5. Anchorages in bottom location of RAC specimens show a resistance similar to that in conventional concrete; however, a greater TC effect is observed in RAC, probably due to the segregation of concrete with

blast furnace slag. Therefore, the current provisions of *fib*-Model Code on casting position can hardly be applied to RAC. However, a proper mix design of the RAC concrete would guarantee a more homogeneous mixture to limit the cast effect of the top bars.

NOTATIONS

a_l	distance of anchored bars to the confining link
A_{st}	cross sectional area of one leg of confining stirrups
B	width of the beam end specimen
BS	bond strength ratio
C	corner bar
Ce	center bar
c_s	clear spacing between anchored bars
c_x	side concrete cover
c_y	bottom concrete cover
d_b	diameter of the anchored bar
d_{sw}	stirrup diameter
f_{cm}	mean concrete strength
f_R	relative rib area (bond index)
f_s	measured bar stress
$f_{s,ex}$	nominal bar stress measured at peak load
$f_{s,tgt}$	target stress developed by the anchorage at failure
f_{stm}	maximum anchored bar stress according to fib-MC2010 formulation
$f_{s\delta L,0.05}$	measured bar stress for a loaded end slip of 0.05 mm
$f_{s\delta UL,0.02}$	measured bar stress for an unloaded end slip of 0.02 mm
f_{um}	mean tensile strength of steel rebars
f_{yk}	characteristic yield strength steel rebars
f_{ym}	mean yield strength steel rebars
H	height of the beam end specimen
k_m	effectiveness factor of confining reinforcement
K_{tr}	stirrup index of confinement
$K_{UL,0.02}$	secant stiffness of the stress vs. slip curve for an unloaded end slip of 0.02 mm
L	length of the beam end specimen
l_b	anchorage length
N	number of tested specimen in each series
n_b	number of anchored bars
n_{st}	total number of confining stirrups along the anchorage length
n_t	number of stirrup's legs crossing the splitting failure surface
P, P_u	applied load, ultimate load
TC	ratio between the maximum bar stress developed by a top bar with respect with that measured in the corresponding bottom cast one
w	crack width
α_2	confinement coefficient provided concrete cover (as expressed by MC2010)
δ_L	slip of the bar loaded end
δ_U	slip of the bar unloaded end

ACKNOWLEDGMENTS

The authors would like to thank the technicians Augusto Botturi, Andrea Delbarba of the Laboratory P. Pisa of the University of Brescia for their know-how and assistance during the laboratory activities of this study. The authors are grateful to the Eng. S. A. Haydar, S. Khoury, and A. Dorici for performing the experimental campaign during the work of their master thesis at University of Brescia. The supports by Alfacciai Group in providing the steel bars and Gatti spa in providing RAC concretes are gratefully acknowledged. A special thank goes to Eng. E. Marchina for the support in the experimental program.

DATA AVAILABILITY STATEMENT

The data that support the findings of this study are available from the corresponding author upon reasonable request.

ORCID

Giovanni Metelli https://orcid.org/0000-0002-4334-4108
John Cairns https://orcid.org/0000-0001-9886-3661

REFERENCES

1. Tepfers R. A theory of bond applied to overlapped tensile reinforcement splices for deformed bars. Chalmers University of Technology, Goteborg, Publ 73/2, 328 pp., 1973.
2. fib. Bond of reinforcement in concrete, Bulletin N.10, state-of-art report, T.G. "bond models". 2000, Convener Ralejs Tepfers, 427 pp., ISBN 978-2-88394-050-5.
3. Cairns J, Jones K. The splitting forces generated by bond. Magazine of Concrete Research. 1995;47(171):153–65.
4. Gambarova PG, Rosati GP. Bond and splitting in bar pull-out: behavioural laws and concrete-cover role. Mag Concr Res. 1997;49(179):99–110.
5. Giuriani E, Plizzari GA. Interrelation of splitting and flexural cracks in RC beams. J Struct Eng ASCE. 1998;124(9): 1032–40.
6. Bamonte PF, Gambarova PG. High-bond bars in NSC and HPC: study on size effect and on the local bond stress–slip law. J Struct Eng. 2007;133(2):225–34.
7. Cairns J, Jones K. (1995) influence of rib geometry on strength of lapped joints: an experimental and analytical study. Mag Concr Res. 1995;47(172):253–62.
8. Metelli G, Plizzari GA. Influence of the relative rib area on bond behaviour. Mag Concr Res. 2014;66(6):277–94. https://doi.org/10.1680/macr.13.00198
9. Giuriani E, Plizzari GA, Schumm C. Role of stirrups and residual tensile strength of cracker concrete on bond. J Struct Eng ASCE. 1991;117(1):1–18.
10. Plizzari GA, Deldossi MA, Massimo S. Transverse reinforcement effects on anchored deformed bars. Mag Concr Res. 1998; 50(2):161–77.

11. Metelli G, Marchina E, Plizzari GA. Effects of the position of confining transverse links on lap strength. Struct Concr. 2022;23(5):2928–41. https://doi.org/10.1002/suco.202100642
12. Cairns J. Top cast effect: influence of bond length on splitting mode failure. Struct Concr. 2022;23(5):2696–709. https://doi.org/10.1002/suco.202100376
13. Moccia F, Fernández Ruiz M, Metelli G, Muttoni A, Plizzari G. Casting position effects on bond performance of reinforcement bars. Struct Concr. 2021;22(3):1612–32.
14. Metelli G, Marchina E, Plizzari GA. Experimental study on staggered lapped bars in fiber reinforced concrete beams. Compos Struct. 2017;179:655–64.
15. fib. Bond and anchorage of embedded reinforcement: background to the fib model code for concrete structures 2010. Bulletin N.72, technical report, T.G. "bond models 4.5". 2014, Convener: John Cairns, 170 pp. ISBN 978-2-88394-112-0.
16. fib. International Federation for Structural Concrete. Model code for concrete structures 2010. Berlin, Germany: Ernst & Sohn; 2013. p. 434.
17. fib. International Federation for Structural Concrete. Draft Model Code for Concrete Structures. 2020.
18. RILEM/CEB/FIP. Recommendation RC 6: bond test for reinforcing steel, 2. Pullout Test. 1978.
19. EN 10080:2005. Steel for reinforcement of concrete – Weldable reinforcing steel – General. European Committee for Standardization.
20. pr EN10080. Steel for the reinforcement of concrete - Weldable reinforcing steel - general. European Committee for Standardization. 2023.
21. EN 1992-1-1. Eurocode 2: design of concrete structures - part 1–1: general rules, and rules for buildings, European Committee for Standardization. 2004.
22. Bony JC, Claude G, Soretz S. 'Comparison of beam tests and pull-out tests', Betonstahl in Entwieklung 58 24 p., also in RILEM BuLletin No. 28. 1972.
23. Cairns J, Plizzari GA. Towards a harmonised European bond test. Mater Struct/Mater Constr. 2003;36(262):498–506.
24. EN ISO 15630-1. Steel for the reinforcement and prestressing of concrete - Test methods - part 1: reinforcing bars, rods and wire (ISO 15630-1:2019). 2019.
25. pr EN 1992-1-1. Eurocode 2: design of concrete structures - part 1–1: general rules, and rules for buildings, bridges and civil engineering structures, European Committee for Standardization. 2021.
26. ASTM A944-10. Standard test method for comparing bond strength of steel reinforcement bars to concrete using beam-end specimens. 2015.
27. Sippel TM, Hofmann J. The beam end test as a test specimen for the bond of reinforcement bars in concrete. 5th international conference of bond in concrete 2022. 2022, University of Stuttgart (Germany), 25-27th July 2022:528-40.
28. EN 12350-2. Testing fresh concrete – slump test. European Committee for Standardization. 2001.
29. EN 14651. Test method for metallic fibre concrete. Measuring the flexural tensile strength, CEN. 2005.
30. EN 12504-1. Testing concrete in structures - part 3: determination of pull-out force, CEN. 2019.

AUTHOR BIOGRAPHIES

Giovanni Metelli
DICATAM, University of Brescia, Via Branze, 43, 25123 Brescia, Italy
mail: giovanni.metelli@unibs.it

John Cairns
EGIS, Heriot-Watt University, Edinburgh UK
j.j.cairns@hw.ac.uk

Giovanni Plizzari
DICATAM, University of Brescia, Via Branze, 43, 25123 Brescia, Italy
giovanni.plizzari@unibs.it

How to cite this article: Metelli G, Cairns J, Plizzari G. A new *fib* Model Code proposal for a beam-end type bond test. Structural Concrete. 2023. https://doi.org/10.1002/suco.202300124